

Electrochemical Characterization of Nitrocellulose Membranes towards Bacterial Detection in Water [†]

Grégoire Le Brun^{1,*}, Margo Hauwaert ¹, Audrey Leprince ², Karine Glinel ³, Jacques Mahillon ² and Jean-Pierre Raskin ¹

¹ Institute of Information and Communication Technologies, Electronics and Applied Mathematics, UCLouvain, 1348 Louvain-la-Neuve, Belgium;

² Laboratory of Food and Environmental Microbiology, Earth and Life Institute, UCLouvain, 1348 Louvain-la-Neuve, Belgium;

³ Institute of Condensed Matter and Nanosciences (Bio and Soft Matter), UCLouvain, 1348 Louvain-La-Neuve, Belgium;

* Correspondence: gregoire.lebrun@uclouvain.be

[†] Presented at the 1st International Electronic Conference on Biosensors, 2–17 November 2020; Available online: <https://iecb2020.sciforum.net/>.

Received: date; Accepted: date; Published: date

Abstract: Paper substrates have shown a high potential for development of cost-effective and efficient point-of-care biosensors, essential for public healthcare and environmental diagnostics. Most paper-based biosensors rely on qualitative colorimetric detection schemes with high limits of detection. To overcome this limitation, technologies that combine paper-based substrates and electrochemical detection are being developed to allow for quantification and achieve better performances. In this work, we explore the potential of dielectric measurements towards electrical detection of whole-cell bacteria in nitrocellulose membranes, a paper-derivative. Impedance spectroscopy was considered to characterize the membranes with and without *Bacillus thuringiensis* cells, used as model micro-organism. To specifically target this bacterial strain, phage endolysin cell-wall binding domain (CBD) encoded by a bacteriophage targeting *B. thuringiensis* were prepared and integrated into the membranes as recognition biointerface. The fluid sample containing the bacteria is conducted in the membrane through passive capillarity, and the bacteria are specifically immobilized in the test zone. Resulting changes of the dielectric properties of the membrane are sensed through impedance changes, highlighting the contribution of ions in the bacterial detection mechanism. This experimental proof-of-concept illustrates the electrical detection of 10⁸ CFU/mL bacteria in low-salinity buffers within 5 min.

Keywords: whole-cell bacterial detection; nitrocellulose membrane; dielectric properties; impedance spectroscopy; parallel plates; interdigital electrodes; endolysins; *Bacillus thuringiensis*

1. Introduction

Access to safe and sufficient water contributes to the development of human communities and the enhancement of economic activities [1]. Frequent water quality testing and diligent water management are crucial to identify, control and prevent ground and surface water pollution. Bacterial detection, e.g., for *Escherichia coli* used as a control of water fecal contamination, most widely uses techniques that include colony count, DNA analysis after polymerase chain reaction (PCR) or enzyme-linked immunosorbent assay (ELISA) [2,3]. While showing high performances (detection limits of 1 CFU/mL), the high-costs, requirements of well-equipped laboratory facilities and high time-constraints (at least several hours per test) associated with these techniques are fueling the interest in the development of simple, portable and low-cost tools suitable for a rapid (<1 h) and

precise detection of pathogens. Moreover, due to the recent sanitary pandemic caused by the infectious SARS-CoV-2 virus, the field of action of point-of-care (PoC) devices was highlighted because it has the ability to answer to the need of mass screening, and in particular to screen the virus presence in water environments. Such a method, referred to as wastewater-based epidemiology (WBE), may provide an effective approach to predict the potential spread of the infection by testing for infectious agents in wastewater, which has been approved as an effective way to obtain information on health disease, and pathogens [4].

Paper analytical devices have emerged as powerful PoC biosensors for the rapid diagnosis of pathogens in applications such as health and environmental monitoring, especially in resource-limited settings [5,6]. In particular, such a simple technology shows high promises to make water analysis accessible to both water scientists and citizen groups, without the need for specific training [7]. The interest in paper as valuable platform for biosensor development is multiple. Indeed, paper has interesting spontaneous microfluidic properties through capillarity and favors the attachment of bioreceptors, usually proteins such as antibodies, to provide specificity towards pathogens. Moreover, it is of low-cost and offers easy manufacturing and disposability. These advantages are already being exploited in current Lateral Flow Assay (LFA) like pregnancy test strips, in which analytes of interest are passively wicked through the test to reach a detection zone where the specific bioreceptors act as immobilizing agents. Current paper-based sensors mostly use optical transduction. They require the use of labels (such as gold nanoparticles, which have an intense red color), conjugated with antibodies to achieve specific detection of the immobilized analytes [8]. The major drawbacks of these devices include the lack of sensitivity as only the top 10- μm depth of the paper contributes to the colorimetric signal due to the opaqueness [9], and the mostly qualitative measure output, together failing to reach the detection limits required to ensure potability of water for the different indicators.

The integration of highly sensitive electronic detection methods with paper-based sensors are attracting approaches to circumvent these drawbacks [10]. Unlike conventional planar biosensors, electrochemical measures profiting from paper-porosity allow for volume detection. Indeed, the bioreceptors are immobilized through the whole pore surface of paper and thus increase the number of interactions with targeted pathogens. To this end, novel ways of designing electronic elements on paper substrates, e.g., by printing common sensors such as interdigital electrodes (IDE), are being explored towards integrated devices with new functionalities [11–13]. IDE are typically used in applications such as moisture monitoring, chemical sensing and biosensing [14,15]. Some works have attempted to accommodate electrical bacteria detection on common LFA, mainly based on charge transfer measurements [16,17]. However, they rely on the use of cumbersome additional redox probes. On the contrary, impedance-based biosensors, utilize the electric field generated by electrode pairs to detect minute impedance changes of the system when bacteria are immobilized through specific interaction with bioreceptors. This provides sensitivity towards label-free bacteria suspensions as they alter the global conductivity and permittivity [18–20]. As no electron transfer occurs in the system, the sensing information is thus mainly contained in the dielectric properties of the system, which can be sensed through material measurement systems like parallel plates, IDE, or other dielectric measurement systems.

One of the key factors affecting the analytical performance of LFA is the bioreceptor used to capture the bacteria in the test zone. The development of protein receptors as alternative to the expensive antibodies commonly used in LFA has been a topic of great interest. Bacteriophages, viruses that specifically infect bacteria, produce lytic enzymes called endolysins. These endolysins contain a cell-wall binding domain (CBD) that shows strong affinity and high specificity towards target bacteria and have therefore been suggested as promising alternative bioreceptors for LFA [21,22].

In this work, we innovate paper-based biosensing by electrically detecting label-free, whole bacterial cells captured in NC membranes using parallel plate electrodes. This common material dielectric measurement system is proposed as a new way of monitoring the permittivity changes caused by whole-cell bacteria immobilized within the porous NC membranes. The obtained results

are substantiated by a planar fringing field electrodes system, composed of Interdigital Electrodes (IDE) directly applied on a single side of the membrane. To gain insights in the physical phenomena causing the electrical detection, comparisons were made with saline solutions and physiological buffers at different ionic concentrations. In these schemes, we take advantage of the natural capillarity of NC membrane to bring bacterial suspensions at the testing zone where the membrane is functionalized with the recently discovered CBDs derived from the PlyB221 endolysin encoded by phage Deep-Blue targeting *Bacillus thuringiensis* [23]. This ensures high binding capacity towards the bacteria. Proof of concepts of the proposed biosensor is substantiated: 10^8 CFU/mL of *B. thuringiensis* are detected in low-conductive buffers.

2. Materials and Methods

2.1. Materials

Nitrocellulose membranes on a polyester backing (UniSart Lateral Flow CN95 Backed, 20 μ m nominal pore size) were purchased from Sartorius (Germany). Phosphate buffered saline (PBS, 0.01 M phosphate, pH 7.4) was purchased from Sigma-Aldrich (USA). Deionized (DI) water was produced in our facilities (conductivity $\sigma = 6.6 \times 10^{-6}$ S/m).

2.2. Biological Procedures

2.2.1. Bacterial Strains and Growth Conditions

B. thuringiensis GBJ002 expressing the Cyan Fluorescent Protein (CFP) was used as proof-of-concept for this study. Bacteria were plated on Lysogeny Broth (LB)-agar plate and grown overnight (O/N) at 30°C. Next, an individual colony was used to inoculate 5 mL of LB and the suspension was incubated O/N at 30°C with agitation (120 rpm). Then, the culture was washed twice with an appropriate buffer (water or diluted PBS) to remove residual LB (centrifugation at $10000 \times g$ for 5 min at room temperature (RT)). The pellet was finally resuspended in the appropriate buffer yielding a bacterial suspension of ca. 10^8 CFU/mL.

2.2.2. Phage Endolysins Expression and Purification

A detailed description of the expression and purification of PlyB221 endolysin, encoded by Deep-Blue, a bacteriophage targeting *B. thuringiensis*, can be found in [23]. Purified CBD derived from the endolysin was fused to a Green Fluorescent Protein (GFP) for fluorescence assays. The protein concentration was adjusted to 1 mg/mL.

2.2.3. Preparation and Characterization of the CBD Biointerface for Specific Bacteria Immobilization

A protocol for optimal biofunctionalization of the NC membranes with endolysin CBD based on simple physisorption was developed (Figure 1). Membranes were prepared by individually depositing and shaking 50 μ L of 1 mg/mL solution of purified CBD on the NC. Membranes were then dried in an oven for 60 min at 37°C followed by desiccation for 30 min at RT to fix the proteins to the membrane. Following desiccation, membranes were washed twice during 2 min with deionized (DI) water to remove proteins in excess. Membranes were wiped, dried and finally stored in a desiccation chamber at RT. Effective binding of specific bacteria to the biointerface was assessed by depositing a droplet of *B. thuringiensis* suspension on the biofunctionalized membranes followed by a washing step (Figure 1); confocal laser scanning microscopy (Zeiss LSM 710) experiments were performed to investigate bacteria immobilization in the membrane depth.

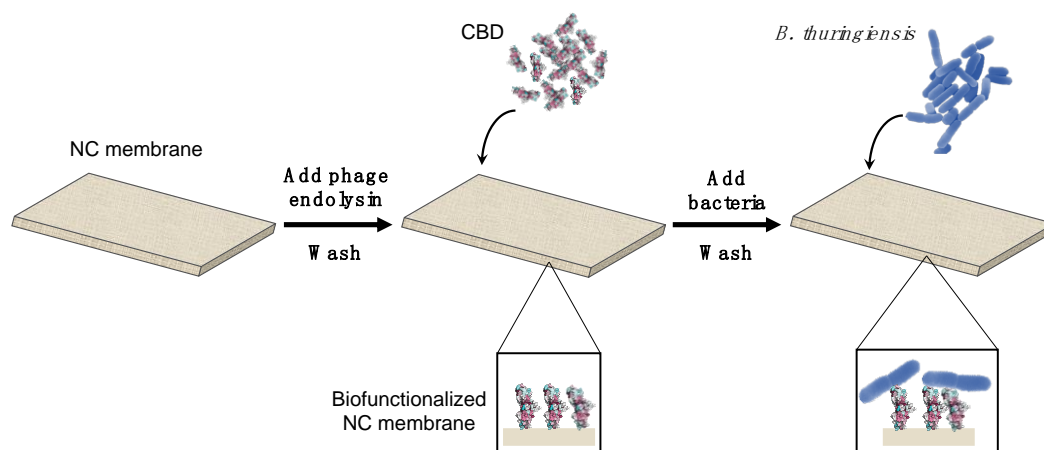


Figure 1. Protocol of the NC membrane biofunctionalization with endolysin CBD and validation of the biointerface through specific capture of *B. thuringiensis* cells. (1) The deposition of the phage endolysin cell-wall binding domain (CBD) in the NC membrane is followed by drying, washing and desiccator steps. (2) The bacteria are then deposited on the membrane and specifically captured by the CBD.

2.3. Parallel Plate Setup and Dielectric Measurement

The nitrocellulose membranes were held between the two parallel plates of the dielectric test fixture (16451B, Agilent, Santa Clara, CA, USA) (Figure 2A), connected to a high-resolution dielectric analyzer (Alpha-A Analyzer, Novocontrol, Germany). The material is stimulated with an AC voltage from 1 kHz to 1 MHz. The material dielectric parameters are derived by knowing the membrane thickness and by measuring its capacitance and dissipation factor. A simple electrical model is used to extract the actual dielectric parameters of the nitrocellulose from the parameters derived for the system composed NC and the polyester backing (Figure 2A). This model considers a double layer capacitance (C_{dl}) in presence of an electrolyte only for the upper electrode, because the backing prevents contact between the charged electrolyte and the lower electrode. The equivalent circuit also considers the nitrocellulose membrane and the backing, both materials being modelled through their capacitive and conductive properties.

2.4. IDE Setup and Impedance Measurement

2.4.1. Interdigital Electrodes Design and Fabrication on NC Membranes

The deposition of IDE on nitrocellulose substrate was conducted using a PVD e-gun evaporation technique. Gold IDE were deposited by applying patterned nickel masks on top of the nitrocellulose membrane. This deposition technique is more cumbersome than screen-printing and inkjet printing techniques which are usually used for deposition of electrodes on paper [24]. However, these have the disadvantage of not allowing precise electrode deposition on chemically untreated nitrocellulose. Hence, PVD is chosen because it allows for precise deposition without inducing variability through additional treatment. The IDE finger width and interdigit gap are 200 μm , which enables the detection of dielectric properties over the whole NC membrane depth ($\sim 140 \mu\text{m}$) [25].

2.4.2. Interdigital Electrodes Impedance Sensing

Figure 2B shows a schematic of the experimental system for IDE measurements and the corresponding electrical model. The IDE were connected through toothless crocodile clips to an impedance analyzer (LCR 4284A, Agilent, USA) through BNC connectors. The impedance spectroscopy measurements were carried out with the LCR, remotely controlled by a computer through the Labview software (National Instruments Corp., USA) to perform an automatic sweep

from 1 kHz to 1 MHz, at voltage amplitude of 20 mV. Before impedance measurement, an open calibration was performed without any electrical contacts between the crocodile clips. The impedance data were extracted in a magnitude-phase data-structure.

The equivalent circuit for IDE measurements, on Figure 2B, incorporates the surfacic phenomenon of double layer capacitance through C_{DL} and the volumic phenomena through C_{air} , R_{air} , C_{NC} and R_{NC} , corresponding to the upper air layer and lower nitrocellulose layer, respectively. Given the width of IDE fingers, the backing is not taken into account (Section 2.4.1).

The double layer capacitance for IDE electrodes in contact with a given solution is given by [19],

$$C_{dl} = \frac{\epsilon_0 \epsilon_{r,sol}}{\sqrt{\frac{\epsilon_0 \epsilon_{r,sol} k_B T}{2 q^2 N_{av} c_{ions} 10^3}}} A_e (N - 1) \tag{1}$$

with C_{dl} the double layer capacitance, k_B the Boltzmann constant, c_{ions} the ion concentration of the solution in which the double layer occurs, $\epsilon_{r,sol}$ the relative permittivity of this solution, A_e the surface per electrode finger and N the number of fingers.

The equivalent capacitances of the nitrocellulose and air volume are given by

$$C_{NC} = K_{cell}^{-1} \epsilon_0 \epsilon_{r,NC} \tag{2}$$

$$C_{air} = K_{cell}^{-1} \epsilon_0 \epsilon_{r,air}$$

with K_{cell} the cell constant and ϵ_r the relative permittivity of the sensed nitrocellulose and air volumes. The cell constant is determined experimentally and incorporates the geometric properties of the IDE [26]. Hence, it does not vary with frequency nor with the electrical properties of the material.

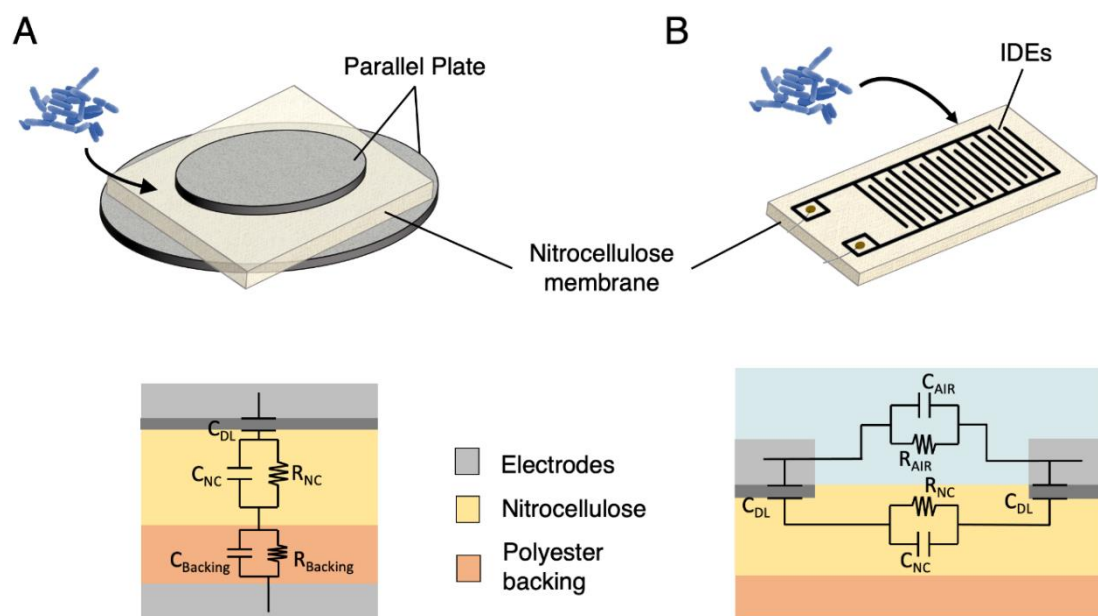


Figure 2. Experimental setups and corresponding electrical models investigated towards bacteria detection in this work. (A) Parallel plate probes are a common material dielectric measurement system. The bacterial sample is deposited on the NC membrane and conducted to the test zone by capillarity. A simple electrical model is proposed to consider the dielectric effect of the polyester backing supporting the NC and the electrical double layer that arises from charge redistribution at the interface between the electrolyte and the probe. (B) Interdigital electrodes are generally used as sensors to monitor impedance changes at the proximity of the metallic fingers, here deposited on an NC membrane. The bacterial samples are applied on top of the IDE-NC sensor. The model does not include the polyester backing as its impact on the impedance seen by the IDE is negligible due to its depth.

2.5. Bacteria Detection in Physiological Buffers

Before depositing bacterial suspensions, PBS solutions diluted $500 \times$ (PBS 1:500) or $1000 \times$ (PBS 1:1000) in DI water were deposited on a previously biofunctionalized membrane. Dielectric or impedance measurements were performed within 5 min with parallel plates or IDE, respectively. Five minutes is a time limit before which it is assumed that the wet impedance has not changed by more than 5% due to drying. Suspensions of 10^8 CFU/mL of stationary-state *B. thuringiensis* resuspended in PBS 1:500 or PBS 1:1000 were then applied on top of the membrane samples with a micropipette (Figure 2A,B) and spread within the membrane due to capillarity, and dielectric measurements were performed.

3. Results and Discussion

3.1. Characterization of the CBD Biointerface

3.1.1. Optical Characterization of the CBD Biointerface

In [22], binding of the CBD to the bacterial cells was assessed in a cell wall decoration assay, which relies on the observation of the uniform adsorption of the GFP-CBD on *B. thuringiensis* cells by fluorescence microscopy, confirming their potential as immobilizing specific probe for LFA biosensor schemes. In [27], we observed a complete and homogeneous distribution of deposited specific proteins (antibodies) in the whole NC membrane thickness, which is promising to capture bacterial cells in the whole volume, hence allowing for volumic electrical detection. Here, we show that, following the developed protocol, GFP-CBD have been successfully deposited in the NC membrane (Figure 3). Confocal microscopy images recorded after the deposition of bacterial suspension and subsequent washing of the membrane, also show specific capture of *B. thuringiensis* by the CBD inside the NC, confirming the potential of CBD as immobilizing probe in paper-based detection schemes. The biofunctionalisation of the substrate with fluorescent bioreceptors also highlighted the NC porous microstructure, allowing to validate experimentally the mean pore size of the membrane (around $20 \mu\text{m}$). The choice of the membrane pore size is mainly motivated by allowing the flow of bacteria to penetrate through the membrane and reach the test zone, avoiding sieving or clogging of the membrane. Regarding the size of *B. thuringiensis* cells, about $0.5\text{--}1.0 \mu\text{m} \times 2\text{--}5 \mu\text{m}$ [28], adding to their penchant for formation of aggregates [29], justify the choice of a large pore diameter membrane.

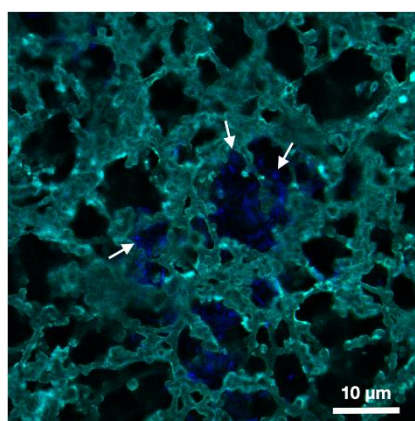


Figure 3. Confocal fluorescence microscopy image of immobilized *B. thuringiensis* cells (blue) in the pores of a CBD-biofunctionalized nitrocellulose membrane (turquoise). The white arrows indicate the presence of captured bacteria on the surface of the membrane pores.

3.1.2. Electrical Characterization of Dry and CBD-Biofunctionalized Nitrocellulose Membranes

The permittivity of a raw nitrocellulose membrane ranges between 1.45 and 1.55 in the range 1 kHz and 1 MHz (Figure 4). The biofunctionalization causes a significant permittivity reduction (at least, within the operation range of the parallel plate setup), ranging from 1.4 at lower frequencies to approximately 1.3 at 1 MHz.

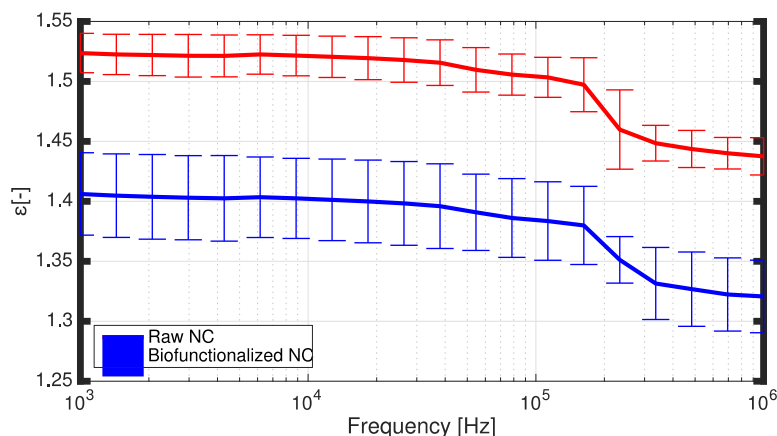


Figure 4. Permittivities of raw and CBD-biofunctionalized nitrocellulose membranes. The biofunctionalization process causes a small decrease in the permittivity. Total number of samples: 7. Error bar: standard error.

Our results show that different parameters can affect the reproducibility of the dielectric measures expressed in the error bars on Figure 4. A first parameter is the inhomogeneity of the membranes. The NC membranes presenting a foam-like structure (Figures 3 and 6), its structural anisotropy and surface inhomogeneity render absolute measures of the permittivity difficult as the solver algorithm assumes that the material under test is homogenous [30]. However, relative measurements are possible between different samples. A second parameter is linked to the biofunctionalization protocol, which can sensibly modify the permittivity of the NC sheets by altering its surface properties. Indeed, under conditions of low humidity reached with the dessicator steps in the protocol, nitrocellulose membranes develop a significant static charge [9], affecting the dielectric measurements. In addition, the presence of a polyester backing (Figure 2) leads to non-effective measures of the dielectric losses (ϵ'') of the substrates. Indeed, the polyester's isolant nature prevents proper and accurate measures of the conductive phenomenon happening in the NC membrane, leading to irrelevant data. Altogether, these limitations make absolute measurements of the system dielectric parameters difficult, while allowing for differential measurements between samples subjected to different conditions.

3.2. Detection of *B. thuringiensis* Cells with the Parallel Plate Setup

Dielectric measurements were carried out with the parallel plate setup to determine the presence of bacteria inside the nitrocellulose membranes. Figure 5A shows a differential bacteria detection measurement performed in low-salinity buffers (PBS 1:1000) by the parallel plate, as explained in Section 2.5. The permittivity extracted from parallel plates measurements shows higher values for the bacteria suspension than for the blank buffer solution in the range from 3 kHz to 700 kHz. Below 3 kHz, the permittivity of the PBS is higher than that of bacterial solutions. When reaching 1 MHz, the permittivities of the membranes filled with PBS or bacterial solutions tend to converge towards a similar value. This convergence continues over the whole frequency range between 1 MHz and 1 GHz (unshown results).

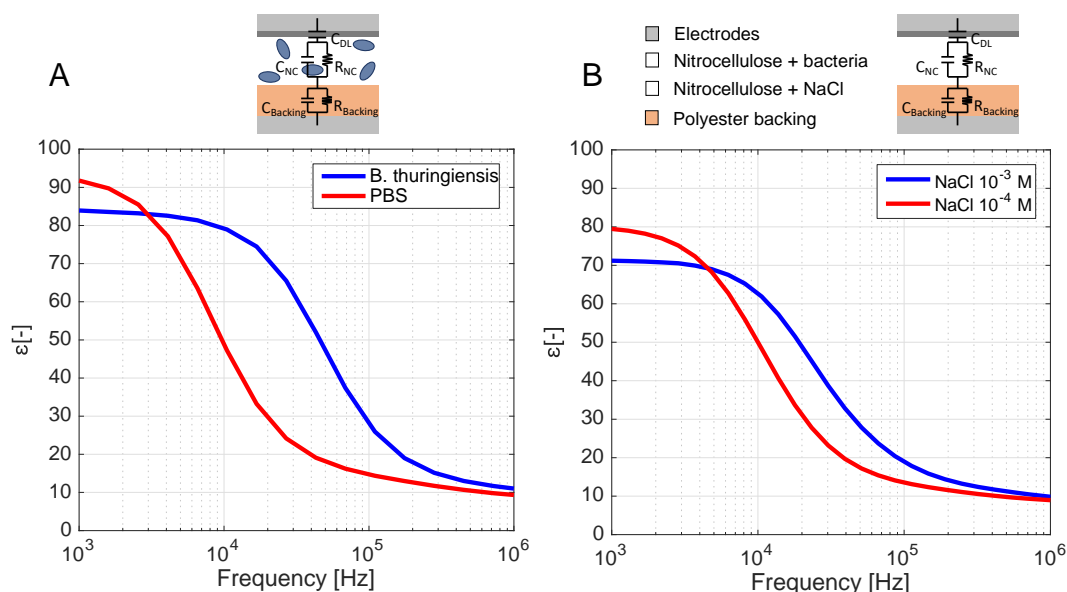


Figure 5. (A) Dielectric permittivity of the nitrocellulose (NC) system as seen by the parallel plate setup. The NC membrane is saturated with PBS 1:1000 (reference buffer) and PBS 1:1000 containing 10^8 CFU/mL *B. thuringiensis* cells. Number of samples: 6. (B) Dielectric permittivity of the system as seen by the parallel plate setup, with different salt concentrations in the nitrocellulose membrane. The behaviour of the saline solution permittivities shows high similarities with the bacterial measurements in PBS (Figure 5A).

To understand the physical origin of the permittivity shift when the nitrocellulose is subjected to bacterial solutions, dielectric measurements on nitrocellulose membranes soaked with saline solutions of different concentrations were performed. In particular, the reference salt concentration, 10^{-4} M NaCl dissolved in DI water, was chosen to roughly model the ionic strength of PBS 1:1000 solutions (Figure 5B), based on PBS ionic content. The broadband behaviour of the relative permittivity changes observed in Figure 5B can be explained by analyzing the dependence of C_{NC} upon the ionic concentration. The dielectric permittivity of electrolyte solutions increasing with the ionic strength [31,32], C_{NC} increases as the ionic concentration increases. This is observed above 3 kHz. However, at lower frequencies (<3 kHz), we observe a different behaviour where the permittivity of more concentrated solutions is lower. This difference could be caused by the specific effects of the double layer, not taken into account by the Windeta software since the permittivity setup is originally designed for the electrical characterisation of dry materials. Unlike the model considered by the algorithm, the ionic solution in the membrane pores supposedly creates a double layer capacitance which dominates the impedance seen by the parallel plates at lower frequencies. The understanding of this effect requires deeper investigations.

The relative shift between both permittivity curves of the saline solutions is caused by the difference in ion concentration (Figure 5B). The relative shift between PBS 1:1000 with and without bacteria, follows a similar pattern (Figure 5A). This suggests that the bacteria detection happens through an increase in ions spread over the whole nitrocellulose volume. The presence of additional ions in bacterial solutions could be caused by centrifugation steps, osmotic shock, or bacterial activity [33,34]. Bacteria releasing ions in the solution accordingly could thus strongly affect the dielectric properties of low-conductive reference buffers such as PBS 1:1000.

The hypothesis of bacterial detection through the augmented ionic concentration caused by bacterial cells in the electrolyte is enforced by a sensitivity measurement with different buffer salinities. Differential dielectric measurements were performed with 10^8 CFU/mL bacterial solutions suspended in PBS 1:500 and PBS 1:1000. Maximum sensitivities were obtained around 4×10^4 Hz for both buffers: a sensitivity of 103% was computed for the PBS 1:500 buffer against 172% for PBS 1:1000

buffers. This highlights the importance of ionic concentration of the reference buffer in the bacteria detection: ions expelled by bacterial cells are less contributing to dielectric changes in highly concentrated buffers than in lower ones. This endorses that the main phenomenon contributing to the detection with parallel plates is the contrast between the initial ionic concentration of the medium and the increased ion concentration when bacteria are present.

3.3. Validation of the Parallel Plate Measurement with the IDE Setup

3.3.1. Gold IDE Deposited on Nitrocellulose Membranes

In order to validate the bacteria detection results obtained with the parallel plate setup, we designed interdigitated electrodes on the NC membranes. Au-IDE were successfully deposited on top of the NC membranes, showing good adherence with the support (Figure 6). The Au-deposited thin-film follows the porous microstructure of the membrane, and showed good conductivity.

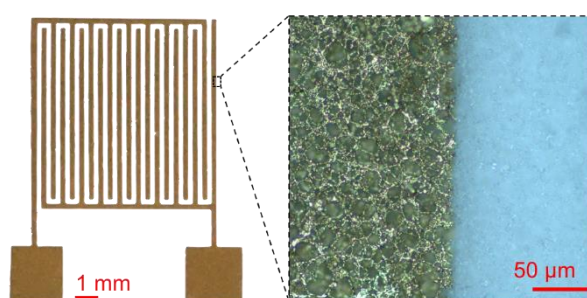


Figure 6. Optical microscopy images of Au-IDE (200 μm of interdigit gap) deposited on a nitrocellulose membrane. The inset is a zoom in image (magnification $\times 20$) of the electrode showing the Au deposition on the membrane surface as well as in the first microns of the membrane thickness due to NC porosity.

3.3.2. Comparison Between Parallel Plate Measurements and IDE Measurements

Impedance measurements were carried out with interdigitated electrodes to substantiate the dielectric measurement results. IDE are among the most commonly used periodic electrode structures for fringing field detection [25]. They offer the advantage that only a single-side access to the test material is required.

The coherence between the outcomes obtained with the parallel plate and the IDE setups is verified through the electrical models. This control consists in extracting the permittivity of the nitrocellulose membrane from the total permittivity seen by the parallel plate. These values are then injected into the IDE model to predict the values of C_{dl} , C_{NC} (Figure 2B), which are then compared to C_{dl} and C_{NC} obtained by direct fitting of the IDE measurements on the equivalent circuit for the IDE.

Table 1 shows ΔC_{dl} and ΔC_{vol} caused by the presence of bacteria, as predicted based on the parallel plate measurement and as deduced from IDE measurements. These differential values have the same order of magnitude. This emphasizes the conclusion that the modeled phenomena, i.e., the double layer capacitance and volumic electrical properties of the nitrocellulose, are predominant in the detection principle.

Table 1. Difference of the double layer and volumic capacitance [F] due to the presence of bacteria as predicted. This difference subtracts the capacitances obtained from the samples without bacteria from the ones with bacteria. Predictions based on the the parallel plate (PP) measurement are compared to results of data fitting from the Interdigital Electrodes results. C_{dl} is approximated at 1 kHz and C_{vol} is approximated at 1 MHz, given that these are the frequencies at which the data-fitting is the most precise.

	ΔC_{dl} [F]	ΔC_{NC} [F]
PP	$+ 1.65 \times 10^{-9}$	$+ 1.3 \times 10^{-14}$
IDE	$+ 1.43 \times 10^{-9}$	$+ 9.9 \times 10^{-15}$

3.4. Perspectives for Future Works

To gain a deeper understanding of the main physical phenomena inducing the bacteria sensing in both measurement systems, the equivalent models of parallel plate and the IDE setups have to be further assessed and compared. Resistive phenomena must be included in the analysis as well. This should allow to compare performances and make well-considered choices of electrode design for bacteria detection in NC membranes.

The detection of bacteria due to the presence of ions presents limitations as it is not very robust in a complex environment with various living organisms that are potential ion-sources, and because it can vary with experimental conditions, procedures and contaminations. Therefore, specificity of the electrical detection can be improved by the use nanoparticles (NPs) to specifically label whole bacterial cells. In [35,36], *E. coli* O157:H7—marker of fecal contamination of water—was detected through enhanced conductance and permittivity changes due to the conjugation of specific graphene or gold NPs to the bacteria. The conjugation of diverse type of NPs with bacterial cells opens perspectives for highly specific bacterial detection, and will be the focus of upcoming works.

5. Conclusions

In this work, a novel method for dielectric characterization of nitrocellulose membranes in presence of bacteria solutions is proposed. Newly discovered endolysin CBD are introduced as specific bioreceptors and successfully deposited inside the nitrocellulose membranes, allowing for bacterial cell immobilization through the whole volume.

Although commonly used for dielectric characterisation of homogeneous materials, our results suggest that the parallel plate setup presents potential for bacterial sensing applications. It allows for a clear detection of 10^8 CFU/mL of *B. thuringiensis* cells without any signal enhancement strategies. The bacteria presence is detected through an overall increase in ions in the PBS 1:1000 solution which modifies the relative permittivity of the NC volume. IDE measures corroborate the parallel plates measurements. Further studies will be conducted towards a deeper understanding of impedance measurements on nitrocellulose membranes with different electrode designs, in order to detect bacteria.

In conclusion, by combining the benefits of NC, novel protein bioreceptors and precise impedance measurements, we obtained promising results towards the development of an affordable, portable and sensitive biosensor with a speed of response under 5 *min*. This creates opportunities in applications that need frequent and rapid pathogen detection, such as the identification of *E. coli* in drinking water. Through appropriate and direct modification of the biointerface, sensing applications could be extended to the detection of various pathogens and viruses as well, which may prove particularly useful in the light of the recent COVID-19 pandemic [37].

Author Contributions: All authors have equally contributed to this work.

Funding: G.L. benefits from a FRIA research fellowship provided by the F.R.S.-FNRS.

Acknowledgments: We thank all the engineers and technicians of the UCL-WINFAB cleanrooms and WELCOME platform for IDE depositions and help in electrical measurements, respectively; W. Xu (IMCN,

UCLouvain) for her help in biofunctionalization protocol development; M.-C. Eloy (LIBST, UCLouvain) for confocal experiments; and researchers from the MIAE lab for protein and bacteria productions.

Conflicts of Interest: The authors declare no conflict of interest. The funders had no role in the design of the study; in the collection, analyses, or interpretation of data; in the writing of the manuscript, or in the decision to publish the results.

References

1. WHO Report. 2019. Available online: <https://www.who.int/news-room/fact-sheets/detail/drinking-water> (accessed on 25 September 2020).
2. Váradi, L.; Luo, J.L.; Hibbs, D.E.; Perry, J.D.; Anderson, R.J.; Orenge, S.; Groundwater, P.W. Methods for the detection and identification of pathogenic bacteria: Past, present, and future. *Chem. Soc. Rev.* **2017**, *46*, 4818–4832, doi:10.1039/c6cs00693k.
3. Lazcka, O.; Del Campo, F.J.; Muñoz, F.X. Pathogen detection: A perspective of traditional methods and biosensors. *Biosens. Bioelectron.* **2007**, *22*, 1205–1217, doi:10.1016/j.bios.2006.06.036.
4. Mao, K.; Zhang, H.; Yang, Z. Can a Paper-Based Device Trace COVID-19 Sources with Wastewater-Based Epidemiology? *Environ. Sci. Technol.* **2020**, *54*, 3733–3735, doi:10.1021/acs.est.0c01174.
5. Parolo, C.; Merkoçi, A. Paper-based nanobiosensors for diagnostics. *Chem. Soc. Rev.* **2013**, *42*, 450–457, doi:10.1039/c2cs35255a.
6. Martinez, A.W.; Phillips, S.T.; Whitesides, G.M.; Carrilho, E. Diagnostics for the Developing World: Microfluidic Paper-Based Analytical Devices. *Anal. Chem.* **2010**, *82*, 3–10, doi:10.1021/ac9013989.
7. Busa, L.S.A.; Mohammadi, S.; Maeki, M.; Ishida, A.; Tani, H.; Tokeshi, M. Advances in Microfluidic Paper-Based Analytical Devices for Food and Water Analysis. *Micromachines* **2016**, *7*, 86, doi:10.3390/mi7050086.
8. Merkoçi, A. Paper Based Sensors. *Compr. Anal. Chem.* **2020**, *89*, 2–464.
9. EMD Millipore. *Rapid Lateral Flow Test Strips—Considerations for Product Development*; EMD Millipore: Burlington, MA, USA, 2013.
10. Nie, Z.; Nijhuis, C.A.; Gong, J.; Chen, X.; Kumachev, A.; Martinez, A.W.; Narovlyansky, M.; Whitesides, G.M. Electrochemical sensing in paper-based microfluidic devices. *Lab a Chip* **2010**, *10*, 477–483, doi:10.1039/b917150a.
11. Jenkins, G.; Wang, Y.; Xie, Y.L.; Wu, Q.; Huang, W.; Wang, L.; Yang, X. Printed electronics integrated with paper-based microfluidics: New methodologies for next-generation health care. *Microfluid. Nanofluidics* **2014**, *19*, 251–261, doi:10.1007/s10404-014-1496-6.
12. Tobjörk, D.; Österbacka, R. Paper Electronics. *Adv. Mater.* **2011**, *23*, 1935–1961, doi:10.1002/adma.201004692.
13. Smith, S.; Land, K.; Joubert, T.-H. Printed Functionality for Point-of-Need Diagnostics in Resource-Limited Settings. In Proceedings of the 2020 IEEE 20th International Conference on Nanotechnology (IEEE-NANO), Montreal, QC, Canada, 29–31 July 2020; Institute of Electrical and Electronics Engineers (IEEE): Piscataway, NJ, USA, 2020; pp. 288–292.
14. Rajapaksha, R.; Uda, M.A.; Hashim, U.; Gopinath, S.C.B.; Fernando, C. Impedance based Aluminium Interdigitated Electrode (Al-IDE) Biosensor on Silicon Substrate for Salmonella Detection. In Proceedings of the 2018 IEEE International Conference on Semiconductor Electronics (ICSE), Kuala Lumpur, Malaysia, 15–17 August 2018; Institute of Electrical and Electronics Engineers (IEEE): Piscataway, NJ, USA, 2018; pp. 93–96.
15. Thivina, V.; Hashim, U.; Arshad, M.M.; Ruslinda, A.; Ayoib, 'A.; Nordin, N.K.S. Design and fabrication of Interdigitated Electrode (IDE) for detection of Ganoderma boninense. In Proceedings of the 2016 IEEE International Conference on Semiconductor Electronics (ICSE), Kuala Lumpur, Malaysia, 17–19 August 2016; Institute of Electrical and Electronics Engineers (IEEE): Piscataway, NJ, USA, 2016; pp. 50–53.
16. Pal, S.; Alocilja, E.; Downes, F.P. Nanowire labeled direct-charge transfer biosensor for detecting Bacillus species. *Biosens. Bioelectron.* **2007**, *22*, 2329–2336, doi:10.1016/j.bios.2007.01.013.
17. Luo, Y.; Nartker, S.; Wiederoder, M.; Miller, H.; Hochhalter, D.; Drzal, L.T.; Alocilja, E.C. Novel Biosensor Based on Electrospun Nanofiber and Magnetic Nanoparticles for the Detection of E. coli O157:H7. *IEEE Trans. Nanotechnol.* **2011**, *11*, 676–681, doi:10.1109/tnano.2011.2174801.
18. Chuang, C.-H.; Shaikh, M.O. Label-free impedance biosensors for Point-of-Care diagnostics. *Point-of-Care Diagnostics New Progresses and Perspectives* **2017**, *03*, 171–201.
19. Couniot, N.; Vanzieleghem, T.; Rasson, J.; Van Overstraeten-Schlögel, N.; Poncelet, O.; Mahillon, J.; Francis, L.; Flandre, D. Lytic enzymes as selectivity means for label-free, microfluidic and impedimetric detection

- of whole-cell bacteria using ALD-Al₂O₃ passivated microelectrodes. *Biosens. Bioelectron.* **2015**, *67*, 154–161, doi:10.1016/j.bios.2014.07.084.
20. Cimafronte, M.; Fulgione, A.; Gaglione, R.; Papaianni, M.; Capparelli, R.; Arciello, A.; Censi, S.B.; Borriello, G.; Velotta, R.; Della Ventura, B. Screen Printed Based Impedimetric Immunosensor for Rapid Detection of *Escherichia coli* in Drinking Water. *Sensors* **2020**, *20*, 274, doi:10.3390/s20010274.
 21. Kong, M.; Sim, J.; Kang, T.; Nguyen, H.H.; Park, H.K.; Chung, B.H.; Ryu, S. A novel and highly specific phage endolysin cell wall binding domain for detection of *Bacillus cereus*. *Eur. Biophys. J.* **2015**, *44*, 437–446, doi:10.1007/s00249-015-1044-7.
 22. Ebai, J.; Ekim, Y.-T.; Ryu, S.; Lee, J.-H. Biocontrol and Rapid Detection of Food-Borne Pathogens Using Bacteriophages and Endolysins. *Front. Microbiol.* **2016**, *7*, 474, doi:10.3389/fmicb.2016.00474.
 23. Leprince, A.; Nuytten, M.; Gillis, A.; Mahillon, J. Characterization of PlyB221 and PlyP32, Two Novel Endolysins Encoded by Phages Preying on the *Bacillus cereus* Group. *Viruses* **2020**, *12*, 1052, doi:10.3390/v12091052.
 24. Liang, T.; Zou, X.; Mazzeo, A.D. A flexible future for paper-based electronics. In Proceedings of the Micro- and Nanotechnology Sensors, Systems, and Applications VIII 2016, Baltimore, MD, USA, 17–21 April 2016; Volume 9836, p. 98361, doi:10.1117/12.2224391.
 25. Mamishev, A.V.; Sundara-Rajan, K.; Yang, F.; Du, Y.; Zahn, M. Interdigital sensors and transducers. *Proc. IEEE* **2004**, *92*, 808–845.
 26. Igreja, R.; Dias, C. Analytical evaluation of the interdigital electrodes capacitance for a multi-layered structure. *Sensors Actuators A: Phys.* **2004**, *112*, 291–301, doi:10.1016/j.sna.2004.01.040.
 27. Le Brun, G.; Raskin, J.-P. Material and manufacturing process selection for electronics eco-design: Case study on paper-based water quality sensors. *Procedia CIRP* **2020**, *90*, 344–349, doi:10.1016/j.procir.2020.02.041.
 28. Lagadic, L.; Caquet, T. *Bacillus thuringiensis*. *Encyclopedia of Toxicology (Third Edition)*; Academic Press: Cambridge, MA, USA, 2014; pp. 355–359, ISBN 9780123864550.
 29. Dorken, G.; Ferguson, G.P.; French, C.E.; Poon, W.C.K. Aggregation by depletion attraction in cultures of bacteria producing exopolysaccharide. *J. R. Soc. Interface* **2012**, *9*, 3490–3502, doi:10.1098/rsif.2012.0498.
 30. Agilent Technologies. *Agilent E4991A RF Impedance/Material Analyzer: Installation and Quick Start Guide (Tenth Edition)*; Agilent Technologies: Santa Clara, CA, USA, June 2012.
 31. Leroy, P.; Weigand, M.; Mériquet, G.; Zimmermann, E.; Tournassat, C.; Fagerlund, F.; Kemna, A.; Huisman, J.A. Spectral induced polarization of Na-montmorillonite dispersions. *J. Colloid Interface Sci.* **2017**, *505*, 1093–1110, doi:10.1016/j.jcis.2017.06.071.
 32. Gavish, N.; Promislow, K. Dependence of the dielectric constant of electrolyte solutions on ionic concentration: A microfield approach. *Phys. Rev. E* **2016**, *94*, 012611, doi:10.1103/physreve.94.012611.
 33. Peterson, B.W.; Sharma, P.K.; Van Der Mei, H.C.; Busscher, H.J. Bacterial Cell Surface Damage Due to Centrifugal Compaction. *Appl. Environ. Microbiol.* **2011**, *78*, 120–125, doi:10.1128/aem.06780-11.
 34. Martinac, B.; Saimi, Y.; Kung, C. Ion Channels in Microbes. *Physiol. Rev.* **2008**, *88*, 1449–1490, doi:10.1152/physrev.00005.2008.
 35. Yao, L.; Wang, L.; Huang, F.; Cai, G.; Xi, X.; Lin, J. A microfluidic impedance biosensor based on immunomagnetic separation and urease catalysis for continuous-flow detection of *E. coli* O157:H7. *Sensors Actuators B Chem.* **2018**, *259*, 1013–1021, doi:10.1016/j.snb.2017.12.110.
 36. Hassan, A.-R.H.A.-A.; De La Escosura-Muñiz, A.; Merkoçi, A. Highly sensitive and rapid determination of *Escherichia coli* O157:H7 in minced beef and water using electrocatalytic gold nanoparticle tags. *Biosens. Bioelectron.* **2015**, *67*, 511–515, doi:10.1016/j.bios.2014.09.019.
 37. Larsen, D.A.; Wigginton, K.R. Tracking COVID-19 with wastewater. *Nat. Biotechnol.* **2020**, *38*, 1151–1153, doi:10.1038/s41587-020-0690-1.

Publisher’s Note: MDPI stays neutral with regard to jurisdictional claims in published maps and institutional affiliations.



© 2020 by the authors. Submitted for possible open access publication under the terms and conditions of the Creative Commons Attribution (CC BY) license (<http://creativecommons.org/licenses/by/4.0/>).